Polymer 119 (2017) 212–223

Contents lists available at ScienceDirect

Polymer

journal homepage: www.elsevier.com/locate/polymer

A composition-morphology map for particle-filled blends of immiscible thermoplastic polymers

Derrick Amoabeng [a, *], David Roell [b], Kendal M. Clouse [b], Brian A. Young [b], Sachin S. Velankar [a, c]

[a] University of Pittsburgh, Dept. of Chemical and Petroleum Engineering, Pittsburgh, PA 15261, USA
[b] Penn State Erie, The Behrend College, Dept. of Plastics Engineering, Erie, PA 16563, USA
[c] University of Pittsburgh, Dept. of Mechanical Engineering and Material Science, Pittsburgh, PA 15261, USA

ARTICLE INFO

Article history:
Received 11 January 2017
Received in revised form
21 March 2017
Accepted 4 April 2017
Available online 5 April 2017

Keywords:
Cocontinuity
Filled polymer blends
Pendular aggregates
Phase inversion
Rheology

ABSTRACT

We explore the effects of adding silica particles to blends of two immiscible polymers, polyisobutylene (PIB) and polyethylene oxide (PEO) across a wide range of compositions, and particle loadings of up to 30 vol %. The silica particles have strong affinity for PEO, and hence, if there is sufficient PEO to fully engulf the particles, a combined phase of particles-in-PEO is formed. We construct a composition-morphology map which reveals two microstructures that are qualitatively different from those seen in particle-free polymer blends: one in which particles are bonded together by small menisci of PEO, and the other in which a highly-filled particles-in-PEO phase percolates throughout the sample. Particles widen the composition range over which co-continuous structures appear. Overall we find that particles affect the morphology greatly when the polymer preferred by the particles (PEO) is in a minority, but only modestly when the preferred polymer is in a majority.

1. Introduction

Immiscible homopolymers are often blended together to realize blends with improved mechanical, electrical, or transport properties [1–3]. In many such applications, the morphology of the polymer blend plays a critical role in determining the properties of the blend, and hence there has been much research on structure development in such blends. This includes mapping out the relationship between morphology and composition, the effect of the relative viscosity or elasticity of the constituents on phase continuity, and exploiting compatibilizers to modify the morphology [4–12]. In this paper, we are concerned with polymer blends that are filled with a solid particulate species. The central question motivating this paper is: how does a particulate filler affect the morphology of an immiscible polymer blend?

Much of the literature on particle-filled polymer blends has been summarized in excellent reviews by Fenouillot et al. [13], Taguet et al. [14], and Filippone et al. [15] and further research in this area continues [16–18]. Most of the existing research has focused on situations in which the particulate filler is present at a low volume fraction, usually less than 5 vol% [13,19–22]. Even at these relatively dilute loadings, remarkable effects have been noted: morphological stabilization (i.e. morphology remaining stable for extended periods under molten conditions) [23–25], an improvement in dispersion (i.e. a finer-scale morphology) [23,26,27], and changes in phase continuity induced by filler [25,28]. Studies at filler loadings exceeding 5 vol% are uncommon [25,29–33], and each of these covers only a narrow range of blend compositions. A comprehensive study of particle effects across the entire composition space remains missing.

In contrast to filled polymer blends, studies of small molecule liquid/fluid/particle mixtures span a much wider range of compositions. Much of this literature comes from oil/water/particle or air/water/particle mixtures, although there has been some research on "model" polymer systems with very low molecular weights as well [34–42]. These studies suggest that the full morphological picture is far more complex than recognized in the filled polymer blends community and there is rich morphological diversity as the particle loading and the ratio of the two liquid phases is varied [43,44]. For illustration, consider for instance a mixture of oil, water, and fully-hydrophilic particles. If the water is in a majority, one obtains a microstructure of oil drops and particles independently suspended

* Corresponding author.
E-mail address: velankar@pitt.edu (D. Amoabeng).

http://dx.doi.org/10.1016/j.polymer.2017.04.009
0032-3861/

in water. If the water is in a minority, the morphology consists of particles suspended inside water drops that are themselves suspended in oil, dubbed a "particles-in-drops" microstructure. If the water is in a very small minority, a completely different structure appears, comprising a network of particles bonded together by small menisci of water. Such a structure has been called a "pendular network" [45] and is analogous to the structure of a sand castle which owes its strength to small water menisci that bind together sand grains [46,47]. These three morphologies appear only when the particles are fully-wetted by the water. On the other hand, if the particles are partially-hydrophobic, the morphologies are altogether different since the particles adsorb at the oil/water interface rather than residing in the water [43,44].

It is immediately interesting to ask whether a similar diversity of morphologies can be realized in filled polymer blends, i.e. when the fluid phases are immiscible polymers rather than oil and water. Indeed at least a few of these morphologies have already been noted in particle-filled thermoplastic blends. For instance, Si et al. [23] noted blends of various polymers in which exfoliated clay platelets adsorbed at the interface of the dispersed phase. Such microstructures are analogous to Pickering emulsions in oil/water/particle mixtures. Many similar examples have been cited in reviews [1–3]. Cai et al. [17] examined blends of polystyrene, polyamide, and TiO_2 particles which were fully-wetted by polyamide. They observed a particle-in-polyamide-in-polystyrene morphology which is analogous to the "particles-in-drops" microstructure mentioned in the previous paragraph [17]. Similar particles-in-drops microstructures have been noted by others as well [48–50]. Bai et al. [39] quenched a mixture of low molecular weight polybutene and polystyrene with silica nanoparticles from a temperature at which the two polymers were miscible to a temperature at which they phase-separated. Spinodal decomposition led to the formation of an interfacially-jammed bicontinuous morphology which is analogous to bijels noted in oil/water/particle mixtures [51]. All these examples suggest that there are at least some common features between the morphology of particle-filled polymer blends and oil/water/particle mixtures. Nevertheless, a comprehensive comparison of filled polymer blends vs. small molecule analogs remains missing, and more specifically, the effects of particles on polymer blend morphology at high particle loading remain poorly-understood.

Motivated by this, we conducted studies of the rheology and morphology of blends of two low molecular weight polymers, polyisobutylene and polyethylene oxide, with particulate filler [45,52]. These polymers were low viscosity liquids under molten conditions (approximately 10 Pa s, which is two to three orders of magnitude lower than the viscosity of conventional molten polymers) and could be mixed without needing polymer processing equipment. Using this model system, we constructed a composition-morphology-rheology map across a wide range of compositions [45].

In this article, we now turn to "real" thermoplastics, i.e. polymers that have both, a high molecular weight, and a high melt viscosity. Our primary concern in this paper is mapping the composition-morphology relationship in particle-filled blends of two immiscible thermoplastic homopolymers, with a focus on the "fully-wetting situation", i.e. the particles have a strong affinity for one of the two polymers. Secondarily we will examine whether their behaviors differ from both, oil/water/particle mixtures as well as from the low-molecular analogs examined previously.

There are good reasons to believe that particle-filled blends of molten thermoplastic polymers will behave differently from similar small-molecule systems. Specifically, the morphology of immiscible polymer blends is determined by two factors, the viscous forces during mixing that seek to mix the two polymers, and the interfacial tension forces that seek to demix the polymers by processes such as coalescence or interfacial coarsening [53]. When filler particles are added, a third factor must be introduced: the affinity of the particles towards one or both of the two polymers. While these same three factors (viscous forces, interfacial tension, particle affinity for one phase or for the interface) are present in oil/water/particle mixtures, their relative "strength" is quite different. The viscosity of molten thermoplastic polymers is many orders of magnitude higher than of oil and water, and therefore viscous forces are much higher in polymer blends than in small molecule mixtures. Moreover, interfacial tension between immiscible polymers is typically an order of magnitude lower than between oil and water, and hence the role of interfacial forces is correspondingly diminished. Thus it is possible that any microstructure that arises due to capillary forces may not survive against high viscous forces. For instance, the pendular aggregate structure mentioned above may be disrupted because virtually all the menisci holding together the particles are broken by viscous forces. Similarly, the particles-in-drops morphology may not survive because the large viscous forces make the mean drop size smaller than the mean particle size. Indeed Premphet and Horanont [31] show excellent examples of polymer blends in which the drops are much smaller than the particles, and a pendular aggregate structure does not survive. Another example comes from Plattier et al. [32] who show that particles prefer to partition into the phase with the higher viscosity regardless of thermodynamics. Thus, merely by changing the relative viscosity of the phases, one can move the particles from one phase to another, or to the interface (if the phases have equal viscosity). Yet another example comes from Dil and Favis [48,54] who showed that when particles are pre-dispersed into a high-viscosity polymer, they tend to stay in that polymer or at the interface even if their thermodynamic preference is for the lower viscosity phase. These authors argue that the kinetics of particle migration play a major role in particle localization in filled polymer blends. These results are in sharp contrast to the common opinion in small-molecule systems that particles adsorb at the interface strongly with no consideration given to viscous forces [55].

Apart from the effects related to high viscosity, we also anticipate significant differences in phase inversion behavior. In oil/water mixtures, phase inversion is usually abrupt (i.e. appears in a narrow composition range, although the actual phase inversion composition may depend on the mixing conditions or surfactant). The morphology on each side of the phase inversion composition comprises spherical drops of oil in water or vice versa. In contrast, blends of two immiscible thermoplastics are often characterized by gradual phase inversion over a wider range of compositions within which co-continuous morphologies appear. At compositions adjacent to the phase inversion composition, highly anisotropic or fibrillar morphologies often appear. How particles affect phase inversion and the morphologies near phase inversion of polymer blends is not known at present. Since the behavior of oil/water/particle mixtures is altogether different, past research on phase inversion on such small-molecule systems [56–59] offers no guidance on what to expect in particle-filled polymer blends.

To summarize the motivation for this paper, small molecule liquid/fluid/particle mixtures show rich morphological diversity as the mixture composition is changed. Macromolecular mixtures may offer similar morphological diversity, yet, the higher viscous forces during thermoplastic blending may induce noteworthy differences. The existing literature on particle-filled polymer blends is overwhelmingly at dilute particle loadings, whereas the effect of filler at higher particle loadings, or across the entire range of ratios of the two polymers, is unknown. The goal of this paper is explore, for the first time, the composition-morphology relationship across a wide range of compositions using a single set of materials.

The materials in this paper were selected to permit clean interpretation of the results. The particles are spherical and not agglomerated, and there are no complications of particle shape, quality of dispersion, clustering, or particle porosity. Moreover the two homopolymers have roughly matched viscosity, and hence the phase-inversion composition is not too far from 50/50 composition, with approximately symmetric behavior on the two sides of phase inversion. Due to this simplicity, we are able to identify the "minimum physics" that arises from the coupling between viscous forces, interfacial tension, and particle affinity for one phase. In that sense, this study serves as a starting point for similar composition-spanning studies with more complex particles, e.g. fumed silica which has fractal-like particle aggregates, or plate-like nanoclay particles, which thus far have only been examined at dilute particle loadings [23,60,61].

The outline of this paper is as follows. Section 2 describes the materials and methods. Section 3 presents the morphologies across a wide range of composition space along with a discussion of the various factors governing morphological evolution, and a comparison with small-molecule analogs. Section 4 summarizes and concludes the paper.

2. Materials and methods

2.1. Materials

Experiments used polyisobutylene (PIB BASF Oppanol B-15, $\rho \approx 0.908$ g/mL, $M_w \approx 75000$ g/mol), polyethylene oxide (PEO Dow Polyox N-10, $\rho \approx 1.1$ g/mL, $M_w \approx 10^5$ g/mol) and fused silica particles (Industrial Powders SS1205, $\rho \approx 2$ g/mL). These particles are polydisperse with unimodal size distribution from 0.5 to 5 μm and the mean diameter is 2 μm. An SEM image of the particles is shown in the Electronic Supplementary Information (ESI), Fig. S1. The dynamic oscillatory viscosity of two polymers obtained from frequency sweep experiments is shown in Fig. S2. Both polymers are shear-thinning, and over a wide range of shear rates, the PEO is roughly 1.35 times as viscous as PIB.

As will be shown later, in many blends, the silica particles are completely engulfed by the PEO, i.e. the silica and PEO form a combined phase. This strongly suggests that the silica particles have a strong affinity for the PEO. We believe that the reason for this affinity is that silica surfaces usually have Si-OH groups which can hydrogen-bond with PEO. In contrast, PIB is much less polar than the silica and is also incapable of hydrogen bonding with silica.

A recent article notes that commercial PEO usually contains a small fraction (~2%) of fumed silica [24]. We have not attempted to test whether that affects the morphology-composition relationships. Given that our blends use filler loadings of at least 10%, we speculate that any effect of fumed silica is dwarfed by effects of the added filler.

2.2. Blend preparation

Blends were prepared using a Brabender Electronic Plasti-Corder model number EPL-V5501. It operates on the counter rotation of two roller blades, which induces strong shear forces for efficient mixing of the blends. The maximum mixer capacity with the roller blades installed is 60 mL. The composition is specified by the three volume fractions denoted ϕ_{PIB}, ϕ_{PEO}, and ϕ_p. This study examines particle volume fractions of $\phi_p = 0$, 10, 20, and 30%, and the PEO:PIB ratios are varied from 4:96 to 88:12. The PIB/PEO/silica ternary blends were prepared in a two-step procedure. The mixer was first preheated to 95 °C, the PIB was added, and allowed to attain the 95 °C mixing temperature for 5 min. The PEO was then added in small increments while blending at 92 rpm for 5 min. A small test sample of PIB/PEO blends was taken out of the mixer for later characterization. Then, silica particles were added, also in small increments, and blending continued for 5 min at same speed. For each sample blend, the amount of material at the end of the mixing process was approximately 40 g. The compositions of the blends studied are listed in Table S1 and also shown on a ternary diagram Fig. S3. The various symbols in Fig. S3 correspond to the different morphologies to be discussed later.

2.3. Characterization

Structural characterization was performed using Scanning Electron Microscopy (SEM-JEOL JSM6510). Prior to preparing samples for SEM, a portion of each sample was immersed in n-octane. Samples with high PIB content fragmented when immersed in octane, indicating that the particles and PEO did not form a percolating phase (this will be discussed in detail later). For samples that fragmented in octane, the fragments were deposited onto a filter paper (Millipore, 0.1 μm pore size) and washed by dripping excess octane onto the filter paper. Upon drying, the filter paper was stuck onto a carbon-tape on an SEM stub. Samples that did not fragment in octane were first compression-molded into discs of about 0.8 mm thickness. They were then cryo-fractured under liquid nitrogen. The fractured discs were allowed to reheat to room temperature without exposure to moisture (since PEO is water-soluble). The fractured surfaces were etched by immersing into octane to remove the PIB. The samples were then were then taped to SEM stubs with the fractured surfaces facing upwards, and supported with conducting copper tape. The samples were then coated using a Pd sputtering target for 90 s at 40 mA. Since PIB is removed by selective dissolution in octane for all samples, only the PEO and particles remain for SEM imaging. Thus the images correspond to either the fragments of PEO and particles remaining when samples disintegrate in octane, or fracture surfaces of PEO-continuous samples that do not disintegrate. In the latter, the removal of PIB with octane leaves the appearance of craters or holes.

A limited amount of optical microscopy was conducted with an Olympus Inverted Microscope using 4×, 20×and 40×objectives. For samples that fragmented in octane, the fragmented dispersed phase was pipetted onto a glass slide and imaged directly. For samples which remain intact in octane, direct observation yielded poor images due to the poor transparency of the semi-crystalline PEO. Accordingly small portions of the sample were melted on a glass slide at 95 °C, and observed immediately on the microscope.

3. Results and discussion

A total of 11 particle-free and 24 particle-containing blends were prepared and characterized by SEM. Fig. S3 shows SEM morphologies of all 35 samples that span across the entire composition diagram. This approach of presenting the data on a ternary composition diagram is different from what is popular in the polymer blends literature which usually represents filler effects in rectilinear form (with the filler loading as the primary compositional variable). The rectilinear form is suitable at low filler loadings. However at the higher filler fractions examined here, the composition of each of the polymer phases reduces significantly as filler is added, making a triangular composition diagram more suitable.

The effects of particles are manifold, and therefore interpreting all of them at once is difficult. To represent the large amount of information in more manageable chunks, we will examine images across specific trajectories in composition space (e.g. change PEO:PIB ratio at fixed particle loading, or vary particle loading at

fixed PEO:PIB ratio). By this approach, several trends in morphological evolution with composition can be identified readily. The following discussion is split into six sections: the first on particle-free blends, the next three on particle effects on the morphology, the fifth on particle effects on phase inversion, and the sixth on comparison with small-molecule analogs.

3.1. Particle free blend

Before discussing effects of particles on the morphology, Fig. 1 first presents the morphological changes with composition in the absence of particles. When PEO is in a small minority, it forms the dispersed phase comprising roughly round drops with a size of a few microns (Fig. 1a). With increasing PEO loading, the PEO drops grow in size but remain mostly spherical (not shown in Fig. 1, but see ESI Fig. S4). At a PEO fraction of 33% (Fig. 1b), PEO is still the dispersed phase but it is increasingly non-spherical, with a large increase in size. This is attributable to a sharp increase in coalescence. At 39% PEO (Fig. 1c), the sample no longer disintegrates completely in octane, and 56% PEO (Fig. 1d), the PEO phase remains completely unfragmented. As will be discussed in Section 3.5, the PIB phase of these two samples is continuous as well, i.e. the blends of Fig. 1c&d have a co-continuous morphology. With further increase in PEO content, the PIB loses continuity and becomes the dispersed phase. The PIB inclusions are large and non-spherical at high PIB content (Fig. 1e) and small and nearly spherical when the PIB is dilute (Fig. 1f).

In summary, the particle-free blends show behavior that is consistent with that expected from the literature: (1) the minority phase tends to form the dispersed phase; (2) phase inversion appears when the two polymers have comparable volume fractions; (3) the morphology appears co-continuous at phase inversion; (4) the size of the dispersed phase increases greatly approaching phase inversion from either side; and finally, (5) the dispersed phase becomes increasingly elongated near phase inversion on either side.

3.2. Effect of PEO:PIB ratio at 10% particle loading

Fig. 2 illustrates the effect of changing the ratio of the polymer phases at a fixed particle loading of 10 vol%. These compositions complement those of Fig. 1. Indeed most of the blends of Fig. 2 were prepared by adding particles to the blends of Fig. 1 and, and hence represent – quite literally – the effect of adding particles to the blends of Fig. 1. We will consider each of these in turn.

Fig. 2a corresponds to a regime of composition space where the PEO volume fraction (3%) is much less than the particle fraction (10%). Despite the superficial resemblance of Figs. 2a and 1a, these

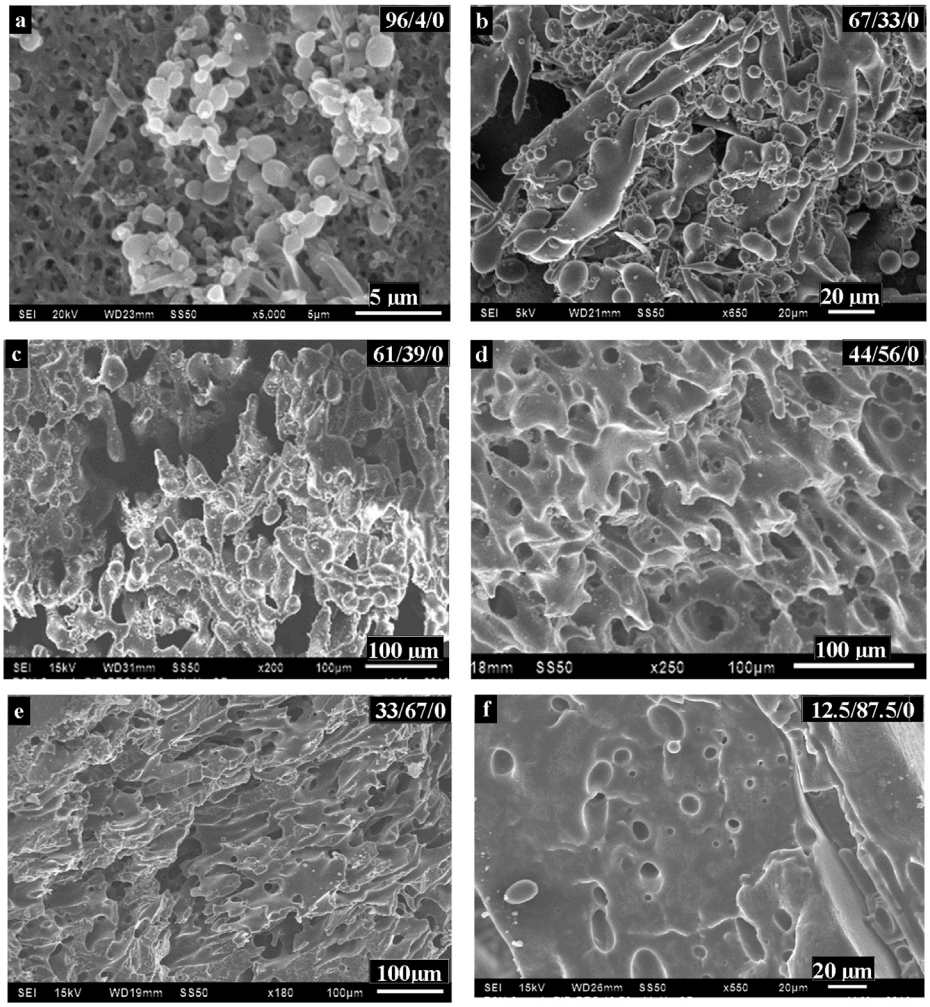

Fig. 1. SEM images of particle-free samples with the PIB/PEO/particle ratios listed at the top right of each image. The corresponding compositions are indicated along the bottom edge of the triangular composition diagram in Fig. 2.

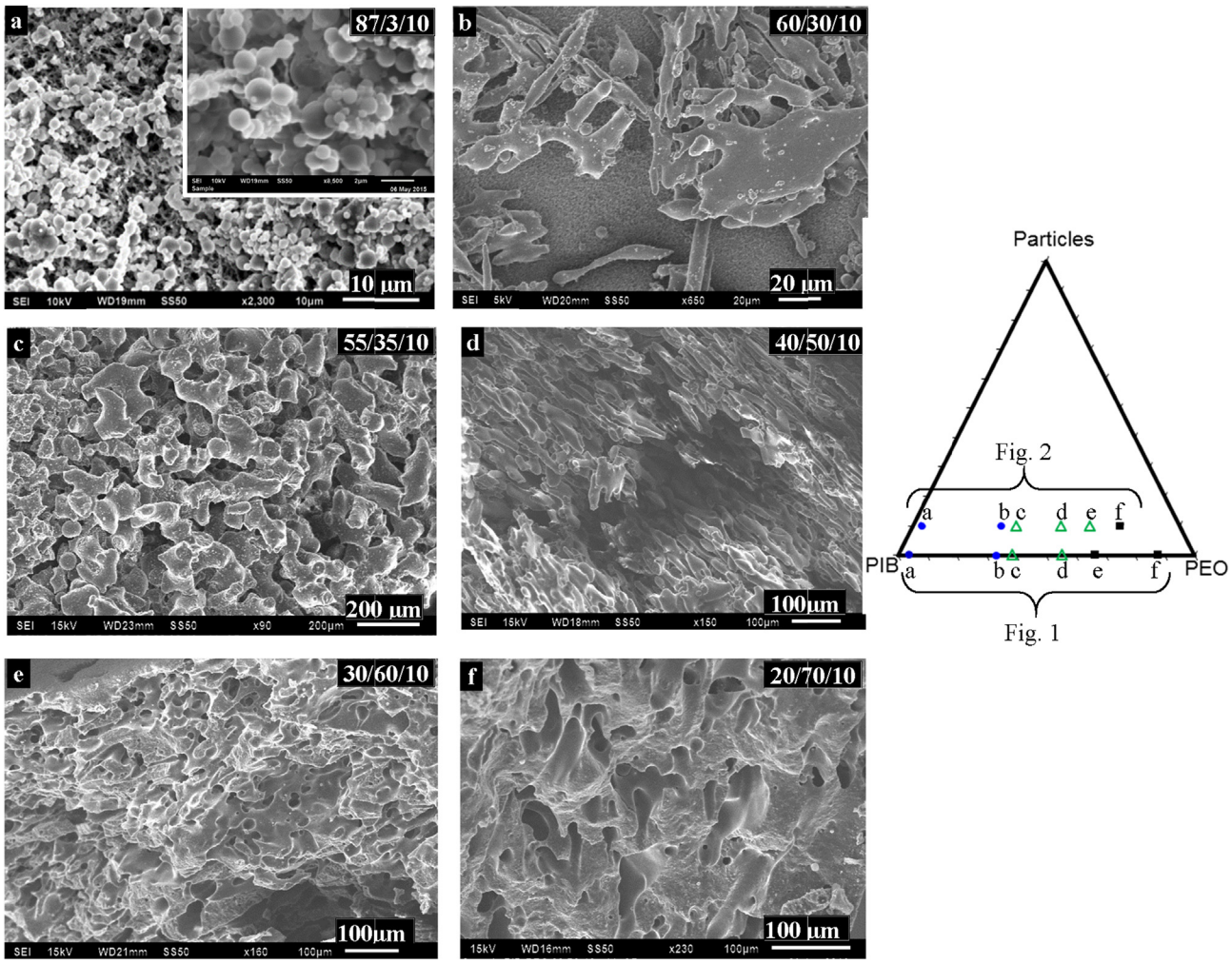

Fig. 2. SEM images of samples with 10 vol% particles. The PIB/PEO/particle ratios are listed at the top right of each image. The triangular composition diagram right shows the compositions of the samples in Figs. 1 and 2.

two morphologies are completely different. In Fig. 1a, the round particles visible are the solidified PEO drops, whereas in Fig. 2a, a majority of the round particles are silica. The inset to Fig. 2a shows a higher magnification view of the sample, and the same inset has been reproduced in the ESI, Fig. S5, in a magnified form for clarity. It is clear from these images that the particles are not separated from each other, but bound to each other by PEO. As mentioned in the Introduction, such a morphology resembles that of a sandcastle where water menisci bind together grains of sand. The literature on wet granular materials [61] makes a distinction between a "pendular" morphology (where each meniscus is hour-glass shaped and binds two particles), and a "funicular" morphology (where a single meniscus binds together multiple particles). Fig. 2a suggests a funicular morphology although occasional pair-wise contacts are evident. It is noteworthy that such a morphology has no analog in particle-free polymer blends nor in filled polymers (where particles are dispersed into a single homopolymer). Such a morphology appears only when particles and a small amount of the preferentially-wetting polymer are both dispersed together.

At all the other compositions in Fig. 2, the PEO fraction greatly exceeds the particle fraction. Since the PEO is completely wetting towards the particles, when it is in large excess, it completely engulfs the particles and hence a silica + PEO combined phase is formed. The changes in morphology with composition are now qualitatively similar to those in Fig. 1, although there are some differences. Fig. 2b consists of a highly elongated dispersed phase, which resembles Fig. 1b, but with a modest increase in the size of the dispersed phase. Fig. 2c also resembles Fig. 1c, however, there is now a significant increase in the size scale of the morphology, i.e. particles induce coarsening, at least at 10% loading. Indeed we have noted previously that addition of particles can sometime accelerate drop coalescence in polymer blends [18,60], an effect that may be analogous to the "bridging-dewetting" mechanism known in the aqueous foams literature [18].

At even higher PEO loadings (Fig. 2d and e, and f) there are no changes in phase continuity as compared to the particle-free samples. Some changes in the degree of orientation are apparent, yet, we note that the samples were prepared by batch compounding (not by extrusion) and hence apparent differences orientation may not be significant since different portions of the sample may have different levels of orientation.

It is noteworthy that in all these blends, particles are present in the PEO phase which is thermodynamically-preferred. This includes blends such as Fig. 2b&c where, both before and after addition of particles, PEO is the dispersed phase. In such blends, since particles are added to a well-dispersed PEO-in-PIB morphology, the particles first encounter the PIB; they must cross the interface to enter into the PEO phase. Unlike observations such

as Dil and Favis [62] and Gubbels et al. [63], such interphase migration appears to be quite fast.

3.3. Capillary aggregates

The compositions of Fig. 2 were selected to parallel those in Fig. 1. However Fig. 2 skipped over one interesting range of compositions, viz. that between Fig. 2a ($\phi_p \gg \phi_{PEO}$) and 2b ($\phi_p \ll \phi_{PEO}$). That composition range, when $\phi_p \approx \phi_{PEO}$, is the topic of this section. Since the discussion in this section revolves around the PEO loading ***relative to*** the particles, it is useful to define the parameter ϱ as [52,64].

$$\varrho = \frac{\phi_{PEO}}{\phi_p} \tag{1}$$

The values of ϱ for all the samples are included in Table S1. Clearly when $\varrho \ll 1$, one expects a pendular/funicular morphology, since the PEO seeks to wet the particles, but there is not sufficient PEO to engulf them completely. On the other hand, at larger values of ϱ, there is sufficient wetting PEO to engulf the particles, and hence a combined particles + PEO phase is formed. This combined phase has an internal particle filling fraction of

$$\phi_p^{combined} = \frac{\phi_p}{\phi_p + \phi_{PEO}} = \frac{1}{1+\varrho} \tag{2}$$

It is clear then that when ϱ is slightly lower than 1, the combined phase is highly filled. For instance, at $\varrho = 0.75$, $\phi_p^{combined} = 0.57$, a filling level that is nearly impossible to blend homogeneously if PEO and particles were to be mixed together by melt blending. At such high filling fractions, the combined phase is internally-jammed, i.e. its rheology is expected to resemble that of a paste (e.g. possessing a high yield stress) rather than a molten polymer (e.g. being viscous or viscoelastic). To validate this idea directly, we examined the rheological properties of the combined particles + PEO phase extracted from three blends with ϱ values of 2.5, 1.45, and 1.25. These measurements, detailed in the ESI Fig. S6 and the discussion on the same page, show that the samples transition from having a liquid-like rheology to solid-like rheology as ϱ decreases. Indeed we also attempted (see ESI) rheological measurements on the combined phases extracted from a sample with $\varrho = 1$. Even at 95 °C (far exceeding the melting point of PEO), this sample had a crumbly consistency indicative of strongly solid-like behavior, and could not be compression molded for rheometry. In a recent study on small-molecule analogs to the present blends, we showed that such solid-like behavior greatly affects the morphology [45]: the dispersed phase takes on the form of irregular "lumps" which cannot be broken under mixing conditions. To our knowledge, this region of composition space – where particle loading is close to the wetting polymer loading– has not been explored in thermoplastic blends, and we do so here.

The effect of ϱ can be illustrated most clearly, by comparing blends with three different values of ϱ (Fig. 3). At ϱ much lower than 1 (e.g. Fig. 3a has $\varrho = 0.16$), there is insufficient PEO to engulf the particles completely, and the particles are bound together by the small menisci of PEO. Fig. 3a suggests that some PEO menisci are pendular (i.e. each meniscus bonds exactly two particles) whereas most are funicular (several particles are held together by a single shared meniscus). Regardless, the morphology is broadly similar to that in Fig. 2a.

Fig. 3e corresponds to a relatively large value of $\varrho = 2$, and hence $\phi_p \ll \phi_{PEO}$. At this composition, there is sufficient PEO to engulf all the particles. Furthermore, the combined phase has $\phi_p^{combined} = 0.33$, i.e. the combined phase is (in a rheological sense) not very concentrated with particles. Accordingly, we expect this combined phase to have liquid-like rheology. Indeed, the corresponding morphology (Fig. 3e), which consists of a smooth (and mostly round) dispersed phase, confirms that the dispersed phase behaves like "normal" liquid drops. This was dubbed a "particles-in-drops" microstructure in the Introduction.

Fig. 3c corresponds to an intermediate value, $\varrho = 0.6$. At this loading, there is barely sufficient PEO to engulf all the particles. Indeed if the particles were fully-engulfed and homogeneously distributed in the PEO, then the combined phase would have $\phi_p^{combined} = 0.625$. This value far exceeds the highest value of 0.44 examined rheologically in Fig. S6, but it even exceeds the value of 0.5, a value at which the combined phase was too crumbly to be molded. At this extremely high value of particle loading, one may therefore expect the combined phase to be highly solid-like. Indeed the appearance of the dispersed phase in Fig. 3c is quite different from Fig. 3e: the interface in Fig. 3c appears irregular due to protruding particles and furthermore, the dispersed phase is highly non-spherical. Previous research on oil/water systems [59,65,66] suggests that the non-spherical shapes appear because the highly concentrated dispersed phase has a yield stress, and the interfacial tension forces are not sufficient to enforce spherical shaped aggregates. Thus the aggregates retain whatever shapes they achieved during the mixing process. Following the literature on wet granular materials [61], such aggregates were dubbed "capillary aggregates" [59]. It is noteworthy that the dispersed phase size in Fig. 3c is much smaller than in Fig. 3e. We believe that this is because capillary aggregates do not coalesce readily, both due to their high yield stress, and because the protruding particles hinder contact of the molten PEO that is on the interior of the aggregates [59]. In contrast, the dispersed phase in Fig. 3e can undergo coalescence like "normal" liquid drops thus resulting in a larger size.

Fig. 3b, d, and e in the right column of Fig. 3 show samples with roughly the same ϱ values as in the left column, but with a higher total dispersed phase fraction, i.e. going from left to right, the particle loading and PEO loading are increased simultaneously. Since ϱ is held nearly constant, the composition (and hence rheology) of the combined phase is almost identical in the left and right columns of Fig. 3. However the much larger amount of combined phase raises the possibility that the dispersed phase may percolate throughout the sample. Indeed the samples of Fig. 3d and f, remain intact upon immersion into octane, i.e. at these ϱ values, the increase in dispersed phase loading (as compared to Fig. 3c and e) was indeed able to induce percolation of the combined PEO + particles phase. In contrast, the sample of Fig. 3b was found to disintegrate when immersed in octane, i.e. the PEO and particles – even at a particle loading of 30% - are not able to create a percolating network. In analogous small molecule mixtures, we and others have noted percolation under similar compositions [52,67], which is useful for fabrication of porous materials by removal of the less-wetting phase [43]. We speculate that the lack of percolation in Fig. 3b is because the much higher viscous stresses in the current thermoplastic polymeric system disrupt the formation of a large-scale network. This point will be reiterated in Section 3.6.

3.4. Effects of particle loading

Fig. 2 discussed the morphological changes when the ratio of the two polymers was changed at a fixed particle loading of 10%. At this relatively low loading, particles significantly affect the morphology (as compared to Fig. 1) only when the PEO loading is less than the particle loading. In contrast, at $\phi_{PEO} > \phi_p$, particle effects were modest. What happens at much higher particle loadings is the concern of this section. Fig. 4 examines a much higher particle loading of 30%. Even at this far higher particle loading however, the

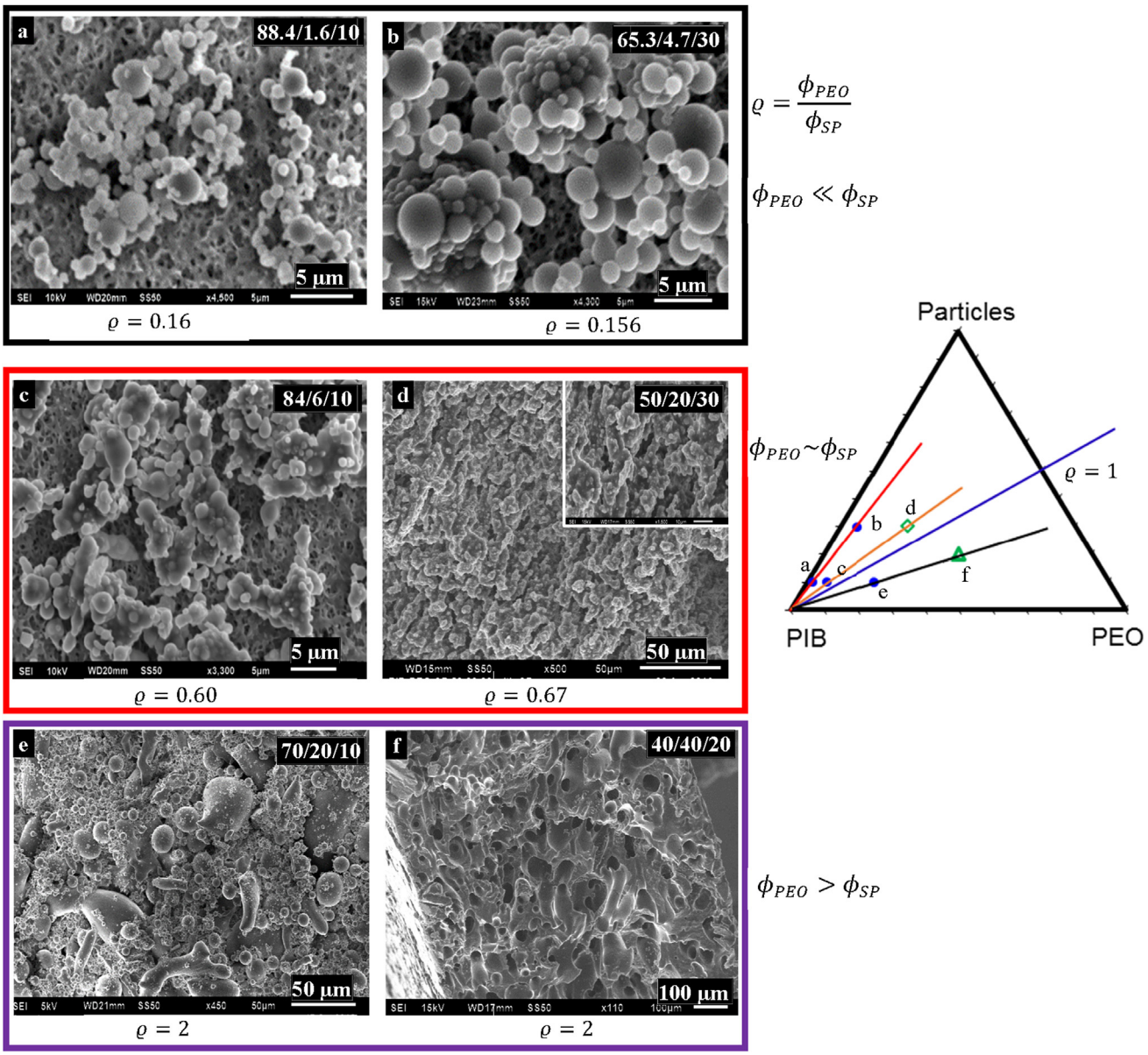

Fig. 3. SEM images of samples where each pair of images in each horizontal row has roughly similar ϱ value. The PIB/PEO/particle ratios are listed at the top right of each image.

qualitative changes in morphology resemble those in Fig. 2: pendular/funicular aggregates a low PEO loading, followed by capillary aggregates, and phase inversion into a PEO-continuous structure. One notable difference is in the nature of phase inversion which will be discussed in Section 3.5.

It is more illuminating to examine the effects of increasing particle loading along composition trajectories at a fixed ratio of the two phases. Accordingly Fig. 5 follows four composition trajectories at PEO:PIB ratios of 22:78, 44:56, 50:50, and 88:12. Since the ratio of the phases is kept fixed, increasing particle loading has two inevitable consequences: increasing the volume fraction of the (PEO + particle) combined phase, and (at sufficiently high particle loadings) endowing the combined phase with a yield stress.

At the ratio of 22:78, the particle-free morphology is PIB-continuous with round PEO drops (Fig. 5c). With increasing particle loading, the size of the combined phase first increases (Fig. 5b), and then the combined phase percolates (Fig. 5a). Since the PIB remains continuous, at this highest particle loading, both phases percolate (see next section).

For the sequence of images at PEO:PIB ratios of 44:56, the most visible effect is on phase continuity: in the absence of particles (Fig. 5f&i), the PEO is highly non-spherical and cocontinuous, however Fig. 5f is on the verge of losing continuity (next section). At higher particle loadings, the cocontinuity appears much better developed and PEO and particles form a continuous phase which percolates throughout the sample. The samples at the PEO:PIB ratio of 50:50 also appear cocontinuous visually (this is verified in the next section).

Finally at the PEO:PIB ratio of 87.5:12.5, PEO + particle phase is continuous, whereas the PIB phase is dispersed. The only apparent effect of particles is a decrease in PIB drop size in Fig. 5j as compared to 5 k.

To summarize, the qualitative changes in morphology are similar at relatively high (30%) loading as at low (10%) loading. In both cases, particles induce large qualitative changes when the PEO content is small, but have only modest effects when the PEO

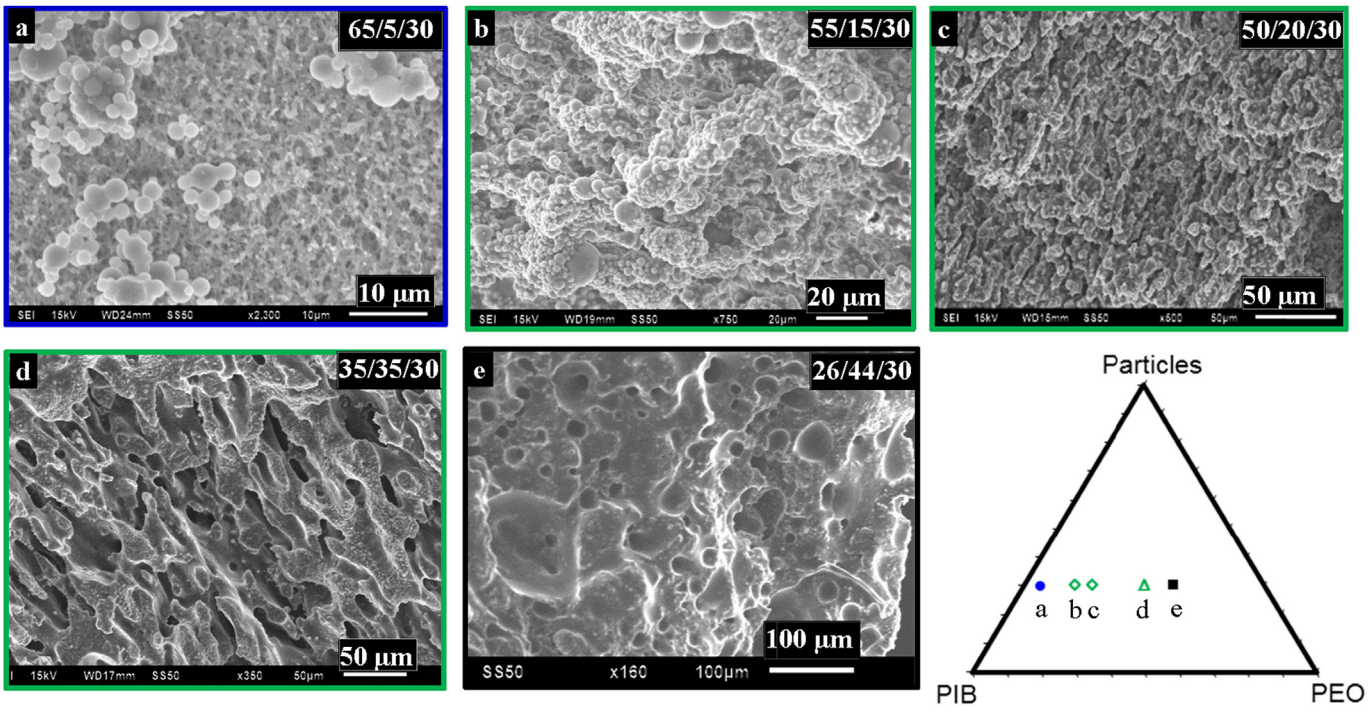

Fig. 4. SEM images of samples with 30 vol% silica. The PIB/PEO/particle ratios are listed at the top right of each image.

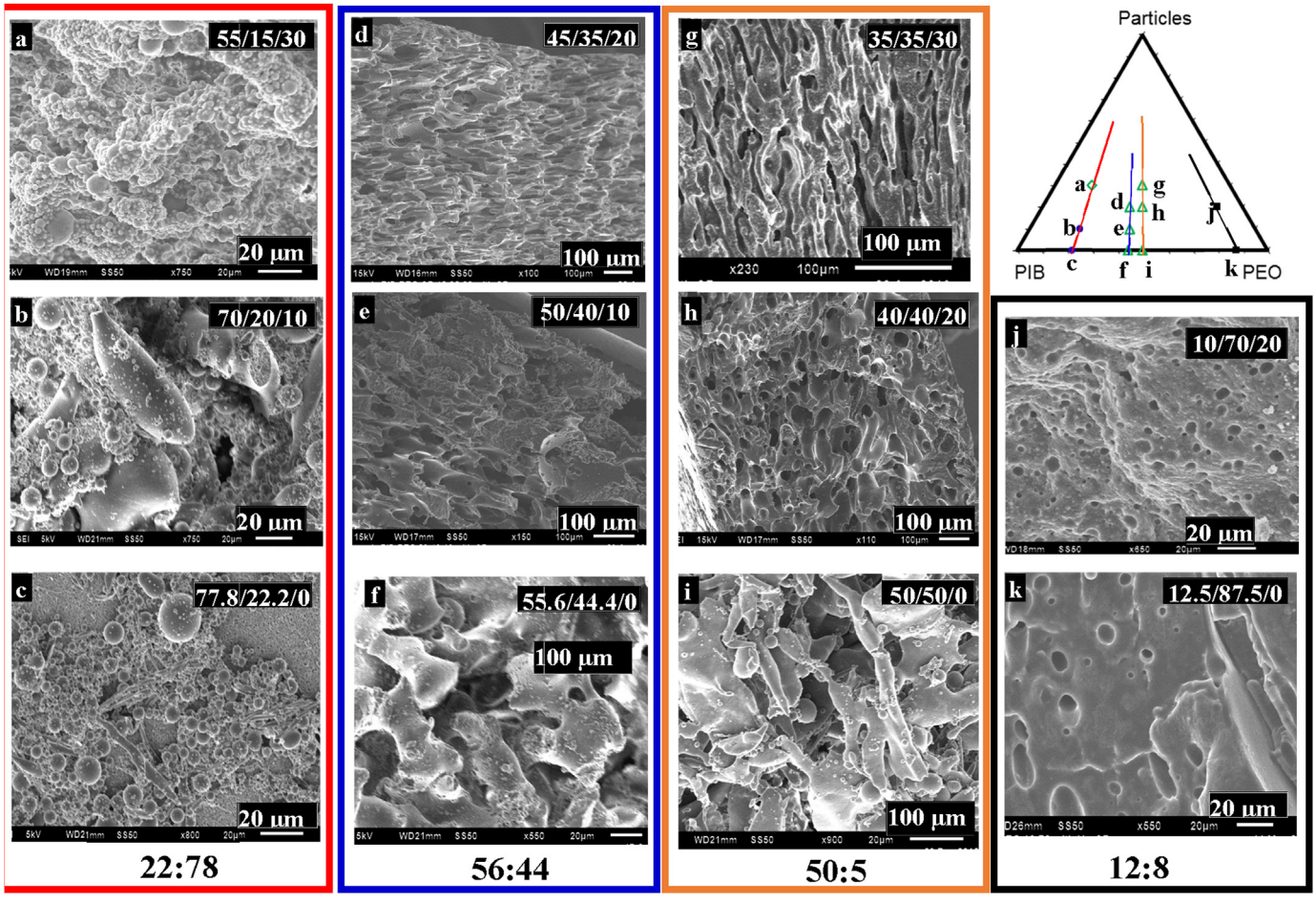

Fig. 5. SEM images showing effects of particle loading at various fixed volume ratios of the two polymers listed along the bottom of each column. The PIB/PEO/particle ratios are listed at the top right of each image. The top right shows the ternary composition diagram with four lines indicating the four volume ratios corresponding to each column of images.

content is large. Particles generally increase drop size, but the results at high PEO loading are not entirely consistent with this.

3.5. Co-continuity, percolation and phase inversion

We have already alluded to changes in phase continuity in the previous sections. Here we will examine phase continuity for all the samples comprehensively. The phase inversion composition has received much attention in the polymer blend community. Various methods including image analysis, solvent extraction, electrical conductivity measurements and rheological measurement have been considered for judging the phase continuity of polymer blends [68,69]. Here we use a combination of image analysis and solvent extraction using octane to judge phase continuity. Samples that fragmented in octane were immediately deemed as having PIB as the only continuous phase. Samples that remained intact in octane, or broke into no more than two or three large fragments, were further quantified as follows. The intact samples were withdrawn from octane, dried, and weighed. The fraction of PIB extracted, f, was calculated as

$$f = \frac{m_{PIB,o} - m_{PIB,f}}{m_{PIB,o}} \tag{3}$$

$m_{PIB,o}$ is the mass of PIB originally present in the sample and $m_{PIB,f}$ is the mass of PIB still remaining in the sample after extraction. In fact these two quantities are not measured separately; instead, the numerator (the change in mass after octane extraction) is measured directly, whereas the denominator is estimated from the known sample composition. Thus $f = 1$ corresponds to extracting all the PIB (implying that the PIB is continuous throughout the sample), whereas $f = 0$ implies that the PIB is entirely trapped within the PEO matrix. In practice, the f values were either in the vicinity of 1 or below 0.6. We occasionally obtained f values somewhat exceeding 1 suggesting that some portion of the PEO may also have been extracted.

The samples were then classified into one of four categories using the following criteria.

3.5.1. PIB-continuous (filled blue circles)

The samples disintegrated when immersed in octane.

3.5.2. PEO-continuous (filled black squares)

The samples remained intact in octane, but the fraction of PIB extracted, f, was less than 0.9.

3.5.3. Cocontinuous (hollow green triangles)

The samples remained nearly intact in octane, the fraction of PIB extracted, f, exceeded 0.9, and the interface appeared smooth.

3.5.4. Capillary aggregate network (hollow green diamonds)

The samples remained intact in octane, the fraction of PIB extracted, f, exceeded 0.9, and the interface appeared rough with particles protruding out.

We note that some points in Fig. 6 that are classified as cocontinuous were on the verge of losing continuity; they fragmented into 2–3 large pieces when immersed in octane. These samples are circled in red in Fig. 6. A comparison of a sample that is on the verge of losing continuity vs those that are "firmly" in the cocontinuous region is shown in Fig. S7.

It must be emphasized that the "cocontinuous" and the "capillary aggregate network" both have two percolating phases. However the ones classified as capillary aggregate networks do not visually resemble the cocontiunuous morphologies common in the polymer blends literature, and indeed they may be stabilized by different mechanisms. Specifically, we pointed out [52] that in analogous small-molecule systems, interfacial tension plays a destabilizing role in cocontinous morphologies, i.e. induces coarsening or breakdown into a dispersed phase microstructure. In contrast, capillary aggregate networks are either unaffected by interfacial tension, or (if the liquid-liquid interface is concave) may even be stabilized by interfacial tension. Indeed Fig. S8 shows that a cocontinuous sample coarsened when held molten at a high temperature for a long time whereas a capillary aggregate network did not show any changes/breakdown.

Examining Fig. 6, it appears that up to 20% particles, the regime of cocontinuity expands due to the addition of particles. More specifically, it is possible to retain continuity of PIB even when it is in a minority (e.g. the sample with a PIB:PEO:silica composition of 30:50:20 is cocontinuous even at 30% PIB). This trend of widening the range of cocontinuity is even more obvious if we exclude the red-circled points in Fig. 6 in which the PEO + particle phase is not robust enough to stay completely intact. However, the "right" edge of bicontinuity appears non-monotonic, i.e. at 30% particles, more PIB is needed to retain PIB phase continuity than at 20% particles. The reasons for this are not clear. We note that at high particle loadings, the combined phase is expected to have solid-like rheology. The difficulty of dispersing such a solid-like phase may be the reason why the combined phase tends to retain continuity.

We sought to develop a simple model to capture changes in phase continuity with particle loading. The essential idea is that since $\phi_{PEO} > \phi_p$ near phase inversion, there is sufficient PEO to entirely engulf the particles. Thus as a first approximation, near phase inversion, the three-phase blend may be treated as an "effectively" two-phase blend of PIB and the combined phase of PEO + particles. In this picture, the particles affect phase inversion in two ways: they increase the volume of the combined phase, and also the viscosity of the combined phase. One may then apply the well-known Paul and Barlow criterion [4] (which accounts for the volume and viscosity of the phases), and derive a criterion for how particle loading affects the phase inversion composition. This approach is illustrated in the ESI and it predicts that particles should increase the PEO:PIB ratio needed for phase inversion. However, the observed shifts in phase continuity do not agree with this prediction even qualitatively (see Supplementary Fig. S9 for a direct comparison). Thus we conclude that treating the ternary mixture as an "effectively binary" mixture is unsuccessful; the effects of fully-wetting particles are more complex than simply increasing the volume fraction and viscosity of the combined phase.

Finally, we note that the sequence of morphologies involved in phase inversion is quite different at low vs high particle fraction. Phase inversion is, by definition, a transition from a morphology in which PIB is the only continuous phase to one in which PEO is the only continuous phase. At low particle loading (lower three schematics in Fig. 6) phase inversion involves transitioning from a particles-in-drops morphology (PIB-continuous) to cocontinuous, and finally to the drops-in-suspension morphology (PEO-continuous). Qualitatively at least, the morphologies on the two sides of phase inversion are symmetric; both consist of roughly spherical drops of one phase in the other. This symmetry is lost at high particle loading because the particles-in-drops morphology does not exist. Instead the pendular/funicular aggregates are the *only* morphology that is PIB-continuous. Thus phase inversion proceeds as per the upper four schematics in Fig. 6: from pendular/funicular aggregates (PIB-continuous), followed by capillary aggregate network and cocontinuous (both of which have two percolating phases), and finally to drops-in-suspension (PEO-continuous). Indeed at even higher particle loading, we speculate that the cocontinuous morphology may disappear as well; capillary

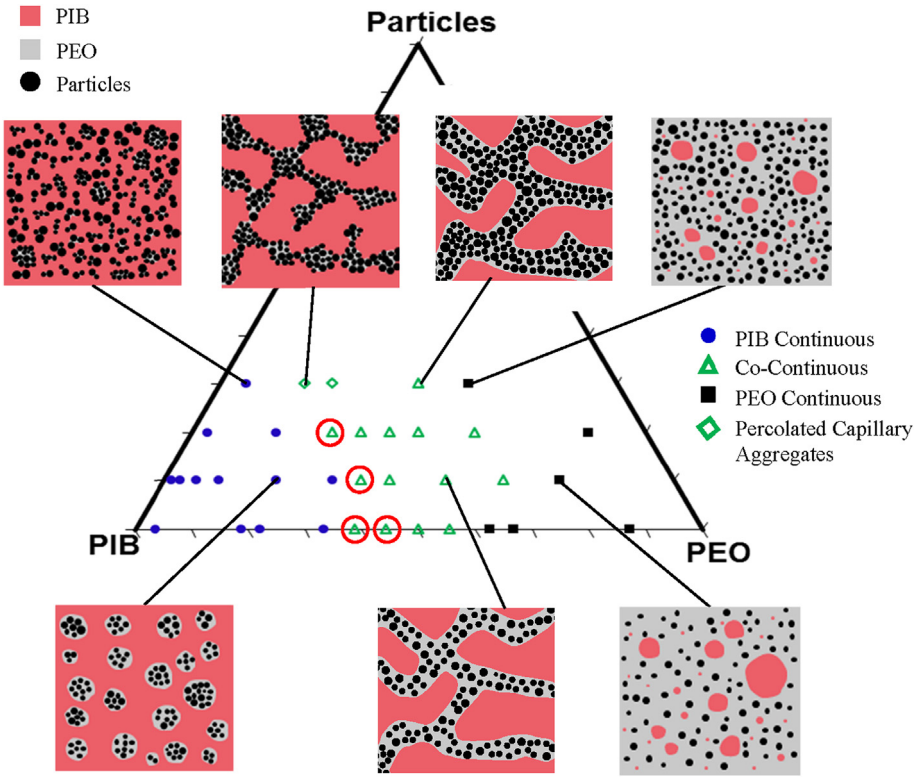

Fig. 6. A classification of phase continuity on the ternary composition diagram. Schematic images of the four different morphologies at 30 vol% particles with particle-in-drops morphology at low particle loading are shown.

aggregate networks will directly invert into the PEO-continuous structure.

3.6. *Differences against small-molecule mixtures*

One of the goals of this research was to identify the ways in which particle-filled thermoplastic blends resemble or differ from both oil/water/particle mixtures as well as blends of immiscible polymers of very low molecular weight (and hence low viscosities). There appear to be broad similarities, and similar morphologies appear in similar regions of composition space [45,52,59]. Two noteworthy differences are apparent. First, in small molecule systems, it is quite easy to realize a pendular/funicular network that percolates across the entire sample [43]. Indeed in oil/water systems, such a network can survive removal of the less-wetting phase even at a particle loading as low as 20% [70]. Here on the other hand, we were unable to create a pendular/funicular network that can survive removal of PIB, even at a particle loading of 30%. We believe that this is because, even though the particle-scale capillary interactions do bind together the particles, the high viscous stresses prevent the association of pendular aggregates into a space-spanning network. A second difference is the existence of cocontinuous or fibrillar morphologies. To our knowledge, a cocontinuous morphology has never been realized in analogous oil/water/particle mixtures with fully-wetting particles. The above results show that there is a range of compositions at which cocontinuous structures appear, and the composition range for cocontinuity becomes wider upon adding particles. Our previous research on blends of very low molecular weight polymers represented an intermediate case in which the particles could stabilize a cocontinuous morphology even though the particle-free blends could not realize a cocontinuous morphology at any composition [52].

4. Conclusion

In summary, we have constructed a morphological map of ternary blends comprising two thermoplastic polymers and one particulate species that is fully wetted by one of the polymers. To our knowledge, the present study is the most comprehensive range of compositions to examine particle effects on the morphology of polymer blends. We show a rich diversity of morphologies, of which two are quite different from the morphologies appearing in binary polymer blends. The first is pendular aggregates in which particles are held together by menisci of the wetting polymer. The second is capillary aggregates comprising inclusions of the wetting polymer that have extremely high particle fillings. Such capillary aggregates can also join together into percolating networks – a morphology that is distinct from conventional cocontinuous morphologies in polymer blends. Finally, a simple model that captures the two main effects of selective filling – that the particles increase the volume and the viscosity of the wetting polymer – does not capture the particle-induced changes in phase inversion composition.

Much of this research was motivated by past observations of analogous small molecule systems, often consisting of particles, oil, and water. Much of the morphology-composition diagram of filled polymer blends is remarkably similar, but with some noteworthy differences: pendular networks appear to be much more stable in small-molecule systems, whereas cocontinuous structures are altogether missing in oil/water systems. We speculate that this is due to the greater capillary forces and smaller viscous forces in oil/water mixtures.

While this paper was purely a study of composition-morphology relationships, it provides the basis for designing filled polymer blends for practical applications. For instance,

applications that require a combination of good transport properties and mechanical robustness can be addressed by cocontinuous morphologies. Particles at a high loading can be employed to reinforce one phase and improve overall mechanical properties, or for instance, change the thermal or electrical conductivity of one phase using metal particles. This paper also serves as the basis for examining more complex situations, e.g. adding plate-like or rod-like particles. If such particles can also be engulfed by one phase, they would be able to induce solid-like behavior at low particle loadings, and hence realize cocontinuous capillary aggregate networks, even at low particle loadings.

Acknowledgements

We are grateful to the National Science Foundation for financial support (NSF-CBET grant no. 0932901 and 1336311). We also acknowledge BASF and Dow Chemicals for making the polymers available for this research. The ternary diagram in the figures were drawn using a publicly available template prepared by David Graham and Nicholas Midgley [71].

Appendix A. Supplementary data

Supplementary data related to this article can be found at http://dx.doi.org/10.1016/j.polymer.2017.04.009.

References

[1] L.A. Utracki, C.A. Wilkie, Springer Link, Polymer Blends Handbook, Springer Netherlands: Kluwer Academic Publishers, Dordrecht, 2014.
[2] C. Harrats, S. Thomas, G. Groeninckx, Micro-and Nanostructured Multiphase Polymer Blend Systems: Phase Morphology and Interfaces, CRC Press, 2005.
[3] M. Folkes, P. Hope, Polymer Blends and Alloys, Springer, London: Blackie Academic & Professional, 1993.
[4] D.R. Paul, J.W. Barlow, Polymer blends, J. Macromol. Sci. 18 (Part C) (1980) 109–168.
[5] U. Sundararaj, C. Macosko, R. Rolando, H. Chan, Morphology development in polymer blends, Polym. Eng. Sci. 32 (1992) 1814–1823.
[6] C.W. Macosko, Morphology development and control in immiscible polymer blends, Macromol. Symp. Wiley Online Libr. (2000) 171–184.
[7] B. Favis, J. Chalifoux, Influence of composition on the morphology of polypropylene/polycarbonate blends, Polymer 29 (1988) 1761–1767.
[8] I. Luzinov, C. Pagnoulle, R. Jérôme, Dependence of phase morphology and mechanical properties of PS/SBR/PE ternary blends on composition: transition from core–shell to triple-phase continuity structures, Polymer 41 (2000) 3381–3389.
[9] J.K. Lee, C.D. Han, Evolution of polymer blend morphology during compounding in a twin-screw extruder, Polymer 41 (2000) 1799–1815.
[10] P. Van Puyvelde, S. Velankar, P. Moldenaers, Rheology and morphology of compatibilized polymer blends, Curr. Opin. Colloid & Interface Sci. 6 (2001) 457–463.
[11] J. Li, B. Favis, Characterizing co-continuous high density polyethylene/polystyrene blends, Polymer 42 (2001) 5047–5053.
[12] H. Li, U. Sundararaj, Morphology development of polymer blends in extruder: the effects of compatibilization and rotation rate, Macromol. Chem. Phys. 210 (2009) 852–863.
[13] F. Fenouillot, P. Cassagnau, J.C. Majesté, Uneven distribution of nanoparticles in immiscible fluids: morphology development in polymer blends, Polymer 50 (2009) 1333–1350.
[14] A. Taguet, P. Cassagnau, J.-M. Lopez-Cuesta, Structuration, selective dispersion and compatibilizing effect of (nano) fillers in polymer blends, Prog. Polym. Sci. 39 (8) (2014) 1526–1563.
[15] G. Filippone, N.T. Dintcheva, D. Acierno, F. La Mantia, The role of organoclay in promoting co-continuous morphology in high-density poly (ethylene)/poly (amide) 6 blends, Polymer 49 (5) (2008) 1312–1322.
[16] G. Wu, B. Li, J. Jiang, Carbon black self-networking induced co-continuity of immiscible polymer blends, Polymer 51 (2010) 2077–2083.
[17] X. Cai, B. Li, Y. Pan, G. Wu, Morphology evolution of immiscible polymer blends as directed by nanoparticle self-agglomeration, Polymer 53 (2012) 259–266.
[18] P. Thareja, K. Moritz, S.S. Velankar, Interfacially active particles in droplet/matrix blends of model immiscible homopolymers: particles can increase or decrease drop size, Rheol. Acta 49 (2010) 285–298.
[19] M.H. Al-Saleh, U. Sundararaj, An innovative method to reduce percolation threshold of carbon black filled immiscible polymer blends, Compos. Part A Appl. Sci. Manuf. 39 (2008) 284–293.
[20] S.S. Ray, M. Bousmina, A. Maazouz, Morphology and properties of organoclay modified polycarbonate/poly(methyl methacrylate) blend, Polym. Eng. Sci. 46 (2006) 1121–1129.
[21] R. Foudazi, H. Nazockdast, Rheology and morphology of nanosilica-containing polypropylene and polypropylene/liquid crystalline polymer blend, J. Appl. Polym. Sci. 128 (2013) 3501–3511.
[22] X.-Q. Liu, R.-Y. Bao, Z.-Y. Liu, W. Yang, B.-H. Xie, M.-B. Yang, Effect of nanosilica on the phase inversion behavior of immiscible PA6/ABS blends, Polym. Test. 32 (2013) 141–149.
[23] M. Si, T. Araki, H. Ade, A. Kilcoyne, R. Fisher, J.C. Sokolov, M.H. Rafailovich, Compatibilizing bulk polymer blends by using organoclays, Macromolecules 39 (2006) 4793–4801.
[24] M. Trifkovic, A.T. Hedegaard, M. Sheikhzadeh, S. Huang, C.W. Macosko, Stabilization of PE/PEO cocontinuous blends by interfacial nanoclays, Macromolecules 48 (2015) 4631–4644.
[25] W. Li, J.G. Goossens, The control of silica nanoparticles on the phase separation of poly (methyl methacrylate)/poly (styrene-co-acrylonitrile) blends, Macromol. Chem. Phys. 214 (2013) 2705–2715.
[26] S.H. Lee, M. Bailly, M. Kontopoulou, Morphology and properties of poly (propylene)/ethylene-octene copolymer blends containing nanosilica, Macromol. Mater. Eng. 297 (2012) 95–103.
[27] H.-s. Lee, P.D. Fasulo, W.R. Rodgers, D. Paul, TPO based nanocomposites. Part 1. Morphology and mechanical properties, Polymer 46 (2005) 11673–11689.
[28] G. Martin, C. Barrès, P. Sonntag, N. Garois, P. Cassagnau, Co-continuous morphology and stress relaxation behaviour of unfilled and silica filled PP/EPDM blends, Mater. Chem. Phys. 113 (2009) 889–898.
[29] S. Steinmann, W. Gronski, C. Friedrich, Influence of selective filling on rheological properties and phase inversion of two-phase polymer blends, Polymer 43 (2002) 4467–4477.
[30] K. Premphet, P. Horanont, Phase structure and property relationships in ternary polypropylene/elastomer/filler composites: Effect of elastomer polarity, J. Appl. Polym. Sci. 76 (2000) 1929–1939.
[31] K. Premphet, P. Horanont, Phase structure of ternary polypropylene/elastomer/filler composites: effect of elastomer polarity, Polymer 41 (2000) 9283–9290.
[32] J. Plattier, L. Benyahia, M. Dorget, F. Niepceron, J.-F. Tassin, Viscosity-induced filler localisation in immiscible polymer blends, Polymer 59 (2015) 260–269.
[33] M.H. Al-Saleh, U. Sundararaj, Electromagnetic interference (EMI) shielding effectiveness of PP/PS polymer blends containing high structure carbon black, Macromol. Mater. Eng. 293 (2008) 621–630.
[34] S. Nagarkar, S.S. Velankar, Rheology and morphology of model immiscible polymer blends with monodisperse spherical particles at the interface, J. Rheol. 57 (2013) 901–926.
[35] P. Thareja, S. Velankar, Particle-induced bridging in immiscible polymer blends, Rheol. Acta 46 (2007) 405–412.
[36] J. Vermant, S. Vandebril, C. Dewitte, P. Moldenaers, Particle-stabilized polymer blends, Rheol. Acta 47 (2008) 835–839.
[37] S. Vandebril, J. Vermant, P. Moldenaers, Efficiently suppressing coalescence in polymer blends using nanoparticles: role of interfacial rheology, Soft Matter 6 (2010) 3353–3362.
[38] J. Vermant, G. Cioccolo, K.G. Nair, P. Moldenaers, Coalescence suppression in model immiscible polymer blends by nano-sized colloidal particles, Rheol. Acta 43 (2004) 529–538.
[39] L. Bai, J.W. Fruehwirth, X. Cheng, C.W. Macosko, Dynamics and rheology of nonpolar bijels, Soft Matter 11 (2015) 5282–5293.
[40] W. Tong, Y. Huang, C. Liu, X. Chen, Q. Yang, G. Li, The morphology of immiscible PDMS/PIB blends filled with silica nanoparticles under shear flow, Colloid Polym. Sci. 288 (2010) 753–760.
[41] Y. He, Y. Huang, Q. Li, Y. Mei, M. Kong, Q. Yang, Morphological hysteresis in immiscible PIB/PDMS blends filled with fumed silica nanoparticles, Colloid Polym. Sci. 290 (2012) 997–1004.
[42] Z.-M. Zou, Z.-Y. Sun, L.-J. An, Effect of fumed silica nanoparticles on the morphology and rheology of immiscible polymer blends, Rheol. Acta 53 (2014) 43–53.
[43] E. Koos, Capillary suspensions: particle networks formed through the capillary force, Curr. Opin. Colloid & Interface Sci. 19 (2014) 575–584.
[44] S.S. Velankar, A non-equilibrium state diagram for liquid/fluid/particle mixtures, Soft Matter 11 (2015) 8393–8403.
[45] T. Domenech, S.S. Velankar, Microstructure, phase inversion and yielding in immiscible polymer blends with selectively wetting silica particles, J. Rheol. 61 (2) (2017) 363–377.
[46] M.M. Kohonen, D. Geromichalos, M. Scheel, C. Schier, S. Herminghaus, On capillary bridges in wet granular materials, Phys. A Stat. Mech. Appl. 339 (2004) 7–15.
[47] J.-P. Wang, E. Gallo, B. François, F. Gabrieli, P. Lambert, Capillary force and rupture of funicular liquid bridges between three spherical bodies, Powder Technol. 305 (2017) 89–98.
[48] E.J. Dil, B.D. Favis, Localization of micro and nano-silica particles in a high interfacial tension poly (lactic acid)/low density polyethylene system, Polymer 77 (2015) 156–166.
[49] L. Elias, F. Fenouillot, J.C. Majeste, P. Cassagnau, Morphology and rheology of immiscible polymer blends filled with silica nanoparticles, Polymer 48 (2007) 6029–6040.
[50] M. Kong, Y. Huang, G. Chen, Q. Yang, G. Li, Retarded relaxation and breakup of deformed PA6 droplets filled with nanosilica in PS matrix during annealing,

Polymer 52 (2011) 5231–5236.
[51] E. Herzig, K. White, A. Schofield, W. Poon, P. Clegg, Bicontinuous emulsions stabilized solely by colloidal particles, Nat. Mater. 6 (2007) 966–971.
[52] T. Domenech, J. Yang, S. Heidlebaugh, S.S. Velankar, Three distinct open-pore morphologies from a single particle-filled polymer blend, Phys. Chem. Chem. Phys. 18 (2016) 4310–4315.
[53] C.L. Tucker III, P. Moldenaers, Microstructural evolution in polymer blends, Annu. Rev. Fluid Mech. 34 (2002) 177–210.
[54] E. Jalali Dil, B.D. Favis, Localization of micro- and nano-silica particles in heterophase poly(lactic acid)/poly(butylene adipate-co-terephthalate) blends, Polymer 76 (2015) 295–306.
[55] B.P. Binks, Particles as surfactants—similarities and differences, Curr. Opin. Colloid & Interface Sci. 7 (2002) 21–41.
[56] B. Binks, S. Lumsdon, Catastrophic phase inversion of water-in-oil emulsions stabilized by hydrophobic silica, Langmuir 16 (2000) 2539–2547.
[57] B. Binks, J. Rodrigues, Types of phase inversion of silica particle stabilized emulsions containing triglyceride oil, Langmuir 19 (2003) 4905–4912.
[58] M. Destribats, S. Gineste, E. Laurichesse, H. Tanner, F. Leal-Calderon, V.r. Héroguez, V. Schmitt, Pickering emulsions: what are the main parameters determining the emulsion type and interfacial properties? Langmuir 30 (2014) 9313–9326.
[59] S.J. Heidlebaugh, T. Domenech, S.V. Iasella, S.S. Velankar, Aggregation and separation in ternary particle/oil/water systems with fully wettable particles, Langmuir 30 (2014) 63–74.
[60] S.P. Nagarkar, S.S. Velankar, Morphology and rheology of ternary fluid–fluid–solid systems, Soft Matter 8 (2012) 8464–8477.
[61] S.M. Iveson, J.A. Beathe, N.W. Page, The dynamic strength of partially saturated powder compacts: the effect of liquid properties, Powder Technol. 127 (2002) 149–161.
[62] E.J. Dil, B.D. Favis, Localization of micro-and nano-silica particles in heterophase poly (lactic acid)/poly (butylene adipate-co-terephthalate) blends, Polymer 76 (2015) 295–306.
[63] F. Gubbels, R. Jérôme, E. Vanlathem, R. Deltour, S. Blacher, F. Brouers, Kinetic and thermodynamic control of the selective localization of carbon black at the interface of immiscible polymer blends, Chem. Mater. 10 (1998) 1227–1235.
[64] T. Domenech, S.S. Velankar, On the rheology of pendular gels and morphological developments in paste-like ternary systems based on capillary attraction, Soft Matter 11 (2015) 1500–1516.
[65] M. Caggioni, A.V. Bayles, J. Lenis, E.M. Furst, P.T. Spicer, Interfacial stability and shape change of anisotropic endoskeleton droplets, Soft Matter 10 (2014) 7647–7652.
[66] K. Boode, P. Walstra, Partial coalescence in oil-in-water emulsions 1. Nature of the aggregation, Colloids Surf. A Physicochem. Eng. Asp. 81 (1993) 121–137.
[67] E. Koos, N. Willenbacher, Capillary forces in suspension rheology, Science 331 (2011) 897–900.
[68] J.A. Galloway, C.W. Macosko, Comparison of methods for the detection of cocontinuity in poly (ethylene oxide)/polystyrene blends, Polym. Eng. Sci. 44 (2004) 714–727.
[69] P. Pötschke, D.R. Paul, Formation of co-continuous structures in melt-mixed Immiscible polymer blends, J. Macromol. Sci. 43 (Part C) (2003) 87–141.
[70] J. Dittmann, E. Koos, N. Willenbacher, Ceramic capillary suspensions: novel processing route for macroporous ceramic materials, J. Am. Ceram. Soc. 96 (2013) 391–397.
[71] D.J. Graham, N.G. Midgley, Graphical representation of particle shape using triangular diagrams: an excel spreadsheet method, Earth Surf. Process. Landf. 25 (13) (2000) 1473–1477.